Journal of Orthopaedic Translation 21 (2020) 146–152

Contents lists available at ScienceDirect

Journal of Orthopaedic Translation

journal homepage: www.journals.elsevier.com/journal-of-orthopaedic-translation

Original Article

Early degeneration of the meniscus revealed by microbiomechanical alteration in a rabbit anterior cruciate ligament transection model

Ting Liang [a,b,☆], Hua-Ye Jiang [a,b,☆], Hai-Tao Li [a,b], Yan-Jun Che [a,b], Hui-Lin Yang [a,b], Kai-Nan An [c], Zong-Ping Luo [a,b,*]

[a] Department of Orthopaedics, The First Affiliated Hospital of Soochow University, Suzhou, Jiangsu, China
[b] Orthopaedic Institute, Medical College, Soochow University, Suzhou, Jiangsu, China
[c] Biomechanics Laboratory, Division of Orthopedic Research, Mayo Clinic, Rochester, MN, USA

ARTICLE INFO

Keywords:
Atomic force microscopy
Energy-dispersive spectroscopy
Histology
Meniscus degeneration
Microbiomechanics

ABSTRACT

Background: The microbiomechanical properties of the meniscus influence the cell response to the surrounding biomechanical environment and are beneficial to understand meniscus repairing and healing. To date, however, this information remains ambiguous. This study aims to characterise the microbiomechanical properties of the meniscus after degeneration in a rabbit anterior cruciate ligament transection (ACLT) model and to analyse the corresponding histology at the macroscale and chemical composition.

Methods: Twenty New Zealand white rabbits were used. Menisci were collected from the knee joints 4 and 8 weeks after the ACLT and from those of the corresponding control groups. The central portions of both medial and lateral menisci were investigated using atomic force microscopy, histological study, and an energy-dispersive spectrometer. The evaluation was conducted regionally within the inner, middle, and outer sites from the top layer (facing the femoral surface) to the bottom layer (facing the tibial surface) in both the lateral and medial menisci to obtain the site-dependent properties.

Results: At 4 weeks after surgery, the dynamic elastic modulus at the microlevel increased significantly at both the top and bottom layers compared with the intact meniscus ($P = 0.021$). At 8 weeks after surgery, the stiffening occurred in all regions ($P = 0.030$). The medial meniscus showed greater change than the lateral meniscus. All these microbiomechanical alterations occurred before the histological findings at the macroscale.

Conclusion: The microbiomechanical properties in the meniscus changed significantly after ACLT and were site dependent. Their alterations occurred before the histological changes of degeneration were observed.

The Translational Potential of this Article: The results of our study indicated that degeneration promoted meniscus stiffening. Thus, they provide a better understanding of the disease process affecting the meniscus. Our results might be beneficial to understand how mechanical forces distribute throughout the healthy and pathologic joint. They indicate the possibility of early diagnosis using a minimally invasive arthroscopic tool, as well as they might guide treatment to the healthy and pathologic meniscus and joint.

Introduction

The meniscus is an important cartilaginous tissue providing stability and smooth articulation within the knee joint, while bearing and transmitting loading during physiological activities [1,2]. The overloading that is induced by joint instability causes meniscus degeneration. Damage or loss of menisci also affects the articular cartilage and increases the risk of osteoarthritis (OA) [3,4]. Meniscus tears are becoming increasingly recognised [5–7] and are associated with loss of biomechanical function [8], joint stability [9], and significant changes in contact pressure and knee joint kinematics, especially in patients with symptomatic OA [10].

Although the macrobiomechanical properties after degeneration have been studied in recent years [11,12], the detailed change at the microscale in the meniscus is still ambiguous. The biomechanical environment

* Corresponding author. Orthopaedic Institute, Soochow University 708 Renmin Road, Suzhou, Jiangsu, 215007, PR China.
E-mail address: zongping_luo@yahoo.com (Z.-P. Luo).
☆ These authors contribute to this paper equally.

https://doi.org/10.1016/j.jot.2019.06.003
Received 21 December 2018; Received in revised form 21 May 2019; Accepted 3 June 2019
Available online 8 August 2019

at the microscale is the level where cells sense and respond to the joint force. The understanding of the microenvironment around cells is essential to determine cellular adaptation. Thus, measurement of microbiomechanical properties in the meniscus will correlate the biomechanical environment with the repair or degeneration response of meniscus cells, thus being useful for the prevention, healing, and repair of meniscus disorders.

Therefore, in this study, we hypothesised that biomechanical properties at a microscale might change after degeneration, accompanied by the observation of histological changes of degeneration. The rabbit anterior cruciate ligament transection (ACLT) model was developed to induce an early degeneration of the meniscus. Atomic force microscopy was used to explore the biomechanical properties at a microscale of the medial and lateral meniscus. Safranin Orange/Fast Green staining and the energy-dispersive spectrometer were used to analyse the meniscus morphology at the macroscale and chemical composition, respectively. The outcomes of this study might be essential to define the cell response to the microbiomechanical environment. They indicate the possibility of early diagnosis using a minimally invasive arthroscopic tool, as well as they might guide the treatment to the healthy and pathologic meniscus and joint.

Methods

Animal model

In this study, all the experimental procedures were approved by the Ethics Committee of the First Affiliated Hospital of Soochow University, approval number ECSU-201700038. The animal experiment complied with the ARRIVE (Animals in Research: Reporting In Vivo Experiments) guidelines and was carried out inaccordance with National Institutes of Health guide for the care and use of Laboratory animals (NIH Publications No. 8023, revised 1978).

Twenty healthy three-month-old male New Zealand white rabbits were used in this study (average weight 2.5 kg). Rabbits were randomly divided into four groups($n = 5$ in each group). Two groups were used as control groups, in which no intervention was performed, and the rabbits were only followed during the experimental time. In the other two groups, rabbits were subjected to surgical induction of joint instability obtained by performing ACLT in the right knee by a trained veterinary surgeon at 2 weeks after adaption and quarantine. Before surgery, rabbits that underwent ACTLwere subcutaneously treated two times (24-hour time interval between the two treatments) with sulfadoxineand trimethoprim 30 mg/kg, morphine 0.1 mg/kg and meloxicam 0.4mg/kg were injected subcutaneously to rabbits. After intramuscular injection of ketamine 1000 40 mg/kg and medetomidine, deep anesthesia was induced and maintained by isoflurane 1-3.5% through respiratory mask. After careful shaving and disinfection (with soap and povidone iodine) of the right knee area, ACLT was performed via lateral approach. The fully rupture of the anterior cruciate ligament was evaluated through the anterior drawer test (manual horizontaldislocation) at the last stage of the surgery before the closure of the capsule of the joint. After surgery, rabbits were not immobilised and allowed to move freely in their individual cages.

Postoperative care

To relieve pain and prevent lameness, the operated rabbits received metoclopramide 0.5 mg/kg subcutaneous injection, Penicillin 2 MU qd and eseridine salicylate 1 cp/day for 3 days, forbuprenorphine 0.01 mg/kg for 4 days and sulfadoxine and trimethoprim 15 mg/kg SC bid (bis in die, it means twice a day) for 9 days. The recovery of the rabbits was monitored by veterinarians every day and all rabbits fully recovered. After 4 and 8 weeks of observation, euthanasia was performed to the experimental rabbits and corresponding menisci, patella and articular cartilage were harvested after a careful bilateral knee dissection.

Histological analysis

Both the control group (C) and transection group (T) were euthanised at 4 (C4 or T4) and 8 (C8 or T8) weeks after ACLT, using an overdose of chloral hydrate. Both the medial and lateral menisci in the right knee were harvested, rinsed with phosphate buffer saline (PBS), and fixed in 10% buffered formalin solution. The central part of the menisci was incubated with 15% sucrose solution at 4 °C until it descended to the bottom of the container, followed by incubation with 30% sucrose solution at 4 °C until tissue descending. The central part of the meniscus was sectioned perpendicularly to the surface to obtain 5-μm-thick layers using a frozen tissue section (CM3050 S; Leica, Nußloch, Germany) and stained with Safranin Orange/Fast Green to assess meniscus histomorphology and glycosaminoglycan (GAG) content. The staining results showed the following: mucins and cytoplasm stained blue-green, nuclei stained black, and sulphated GAG stained red. Histological images were obtained using a binocular microscope (XSP-2CA; Shanghai optical instrument factory, Shanghai, China) at a magnification of 25 × . Red staining was semiquantitatively analysed using ImageJ (NIH, MD, USA). We analysed the entire meniscus cross section and obtained the average GAG content.

Energy dispersive x-ray spectrometry

Samples were critical point dried, gold sputter coated, and then fixed to specimen mounts with silver paint. The analysis was performed on the meniscus cross section at 15 kV using a scanning electron microscope (Quanta 250; FEI, OR, USA) connected to an energy dispersive x-ray spectrometry (EDS) (Team EDS; EDAX INC, NJ, USA).

Micromechanical testing

Atomic force microscopy (Dimension ICON; Bruker, WI, USA) was used in the present study to measure the elastic modulus at a microscale. The central part of the meniscus was sectioned into 20- to 30-μm-thick layers using the frozen tissue section microtome (CM3050 S; Leica). The microbiomechanical testing was conducted using a spherical tip with a borosilicate glass sphere at a diameter of 5 μm gluing onto the V-shaped silicon nitride cantilever at a spring constant of 0.06 N/m (Bruker). During the testing, meniscus tissues were immersed in 0.15 M PBS (pH = 7.4) to maintain a physiological environment. The sample area of 15 μm × 15 μm was scanned at a frequency of 3 Hz. The following equation based on Hertz's law [13,14] was used to calculate the meniscus stiffness:

$$E = \frac{\sqrt{\pi}}{2}\left(1 - \upsilon^2\right)\frac{S}{\sqrt{A}} \quad [1]$$

where E is Young's modulus, υ is Poisson's ratio (0.04 for meniscus, according to a previous study [15]), S is the contact stiffness (the slope of the initial part of the unloading regime of the load-indentation curve), and A is the projected area of the spherical indentation.

Because the elastic modulus of the meniscus may vary in different sites, the cross section was divided into nine scanning areas from inner to outer and from top to bottom, as shown in Figure 1. The histogram was fitted by a Gaussian curve, and the peak of the corresponding Gaussian distribution curve was considered as the most probable modulus.

Statistical analysis

All data are provided as the mean ± standard deviation. Statistical analysis was performed using the SPSS 13.0 software package (IBM, NY, USA). Significant differences between the study groups were calculated

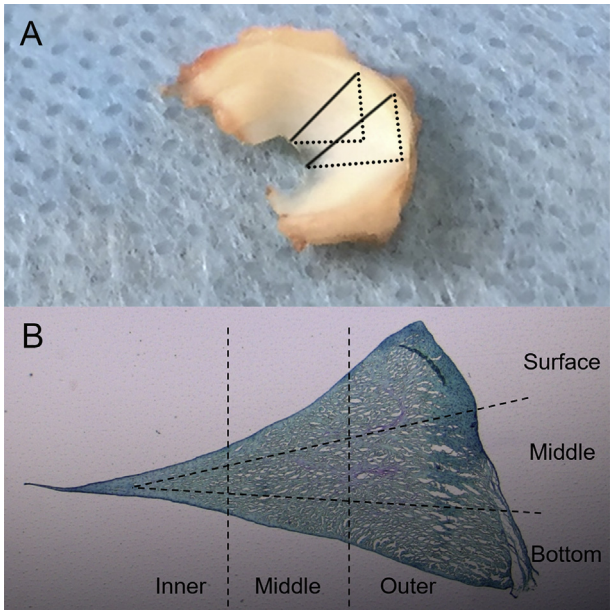

Figure 1. (A) The schematic of the study region and central portion of the meniscus; (B) the schematic of different scanning sites in the meniscus cross section.

using two-way analysis of variance with Fisher's partial least squares difference to analyse the combined influence of the degeneration process and region. Statistical significance was set at $P < 0.05$.

Results

Typical photos of both the lateral and medial meniscus from the control groups and transection groups are shown in Figure 2. No significant damage or tear was observed in the rabbits' medial or lateral meniscus at 4 and 8 weeks after surgery.

The representative histological sections of intact and degenerated menisci are shown in Figure 3. No significant alteration was observed in the T4 groups compared with the C4 group. The red area was more widespread in the T8 group compared with the C8 group in the inner portion of the cross section. The semiquantitative analysis also showed a significant increase in red coverage after transection for 8 weeks ($P = 0.021$).

The calcium and phosphate element content in the meniscus section were measured by the energy-dispersive spectrometer for both the control and transection groups (Figure 4). No significant difference was observed in calcium content between the control and transection groups (Figure 4 (A)). Medial and lateral menisci within each group also showed no significant difference in calcium content. However, the phosphate content significantly increased in the T4 group compared with the C4 group ($P = 0.016$) and in the T8 group compared with the C8 group ($P = 0.020$) (Figure 4 (B)). However, there was no difference between medial and lateral sides within each group.

The representative frequency histograms of dynamic elastic modulus in the top middle site of the medial meniscus are shown in Figure 5. The Gaussian curve peak in the transection groups occurred at a significantly higher modulus compared with that in the control groups. In addition, the modulus distributions of the transection groups were apparently larger than those of the control groups.

The average elastic modulus from different sites within the meniscus section is shown is Figure 6. The scanning position and transection surgery significantly influenced the microstiffness. In the top layer in Figure 6(A), the T4 and T8 groups stiffened within the whole layer compared with the C4 ($P = 0.034$) and C8 ($P = 0.006$) groups, respectively. No significant difference in the control groups was observed between medial and lateral menisci. However, a significant difference was observed between two sides in the whole top layer ($P < 0.001$) in the T4 group, while a significant difference was observed within the inner ($P = 0.031$) and middle ($P = 0.009$) region of the T8 group.

In the middle layer in Figure 6(B), the menisci of the T8 group were stiffer than those of the C8 group ($P < 0.001$), whereas no significant difference was observed between the C4 and T4 groups. The C4 and C8 groups showed no difference between medial and lateral menisci, and the T4 group displayed significant difference between two sides in the whole middle layer ($P < 0.05$). Furthermore, the T8 group exhibited a significant difference between two sides in the inner ($P = 0.027$) and outer ($P = 0.006$) regions.

In the bottom layer in Figure 6(C), the dynamic elastic modulus of the transection groups increased significantly compared with the control groups in all regions ($P < 0.001$). However, the significant difference between medial and lateral menisci was only observed in the outer ($P = 0.016$) and inner region in the T4 and T8 groups, respectively ($P = 0.039$).

Discussion

In the present study, the biomechanical alteration at the microscale of the meniscus was investigated to evaluate the early degeneration of the

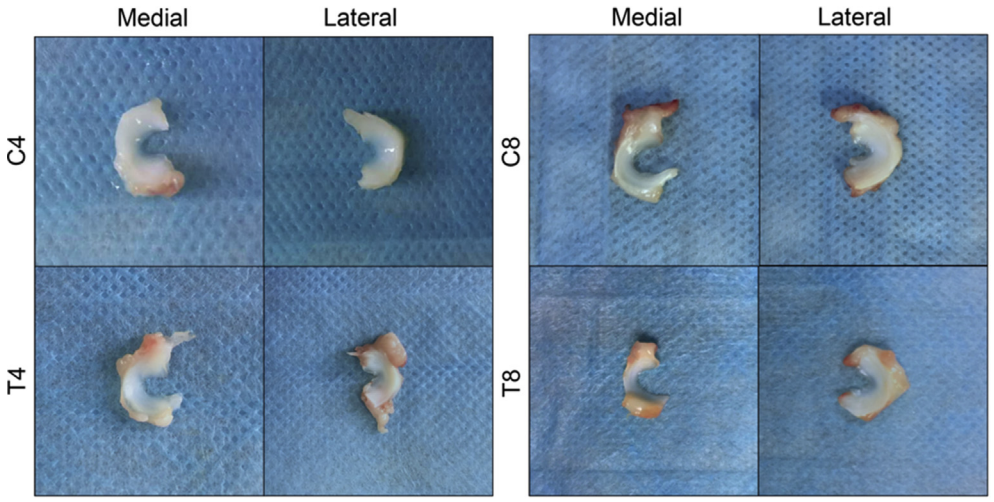

Figure 2. The representative photos of both intact menisci (control groups: C4 and C8) and degenerative menisci (transection groups: T4 and T8). No significant damage or tear was observed in the rabbits' medial or lateral meniscus at 4 and 8 weeks after surgery.

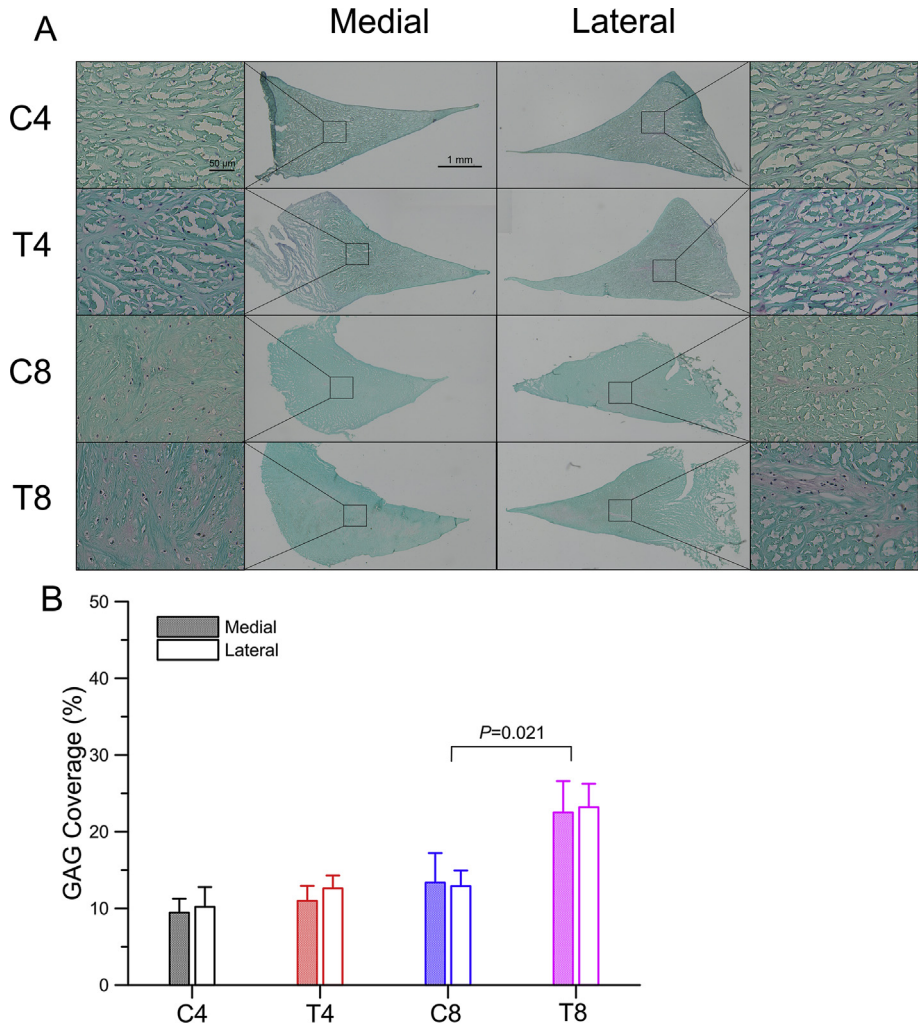

Figure 3. (A) The representative Safranin-O/Fast Green staining images; (B) mean GAG coverage of the meniscus in the control and transection groups (n = 5, mean ± SD). GAG = glycosaminoglycan; SD = standard deviation.

knee joint after ACLT. The regional variations among different scanning sites in both lateral and medial sides were observed by atomic force microscopy. The rabbit ACLT model has been widely used to obtain changes in menisci owing to OA [12,16,17], and to simulate early OA in humans [18]. The experimental study [11,12] and theoretical study [19,20] at a macroscale on the mechanical property of menisci have been previously performed. Between molecular alterations and macromechanical alterations, the local microbiomechanical environment plays an important role in modulating cellular response [21]. However, studies on the biomechanics at the microscale or nanoscale are scarce [13]. At present, complete or partial meniscus removal in the current clinical practice leads to degenerative changes within the joint [22]. Thus, it is necessary to investigate the detailed change of the meniscus in early OA before significant injuries occur, which can be evaluated by ultrasonography [23]. This study measured variations at a microscale in the meniscus section, which is important in strategies of preventing damage and tissue engineering.

Histological analysis revealed an increase in GAG content after degeneration (Figure 3), which was in accordance with previous studies [12,24,25]. At 4 weeks after ACLT, no significant change in GAG content was observed, which is not in accordance to the modulus alteration in this study. This discrepancy indicated that the microbiomechanical property might occur before the macrodegenerative signs. The results may attribute to the damage that led to a loss of mechanical resistance of the menisci. The following increase in the GAG content was attributed to an attempt to compensate for the loss of mechanical resistance. It corresponds to previous studies. However, the correlation between the GAG content and modulus within the menisci was also discrepant among recent studies [12,13,26–28]. Moreover, GAG distribution in the axial direction was not uniform from anterior to posterior region; thus, the comparison of GAG content in the cross section in the central part should be more precise and cautious. Therefore, further examination of the GAG content is required to evaluate how chemical changes affect biomechanical properties.

Calcium or phosphate deposition may be associated with the low compliance of collagen fibrils and the biomechanical properties of collagen fibrils in OA cartilage [29,30]. Although the content of calcium and phosphate (less than 3%) was relatively low in the total composition, this content could still be used for both qualitative analysis and evaluation of the difference between the control and transection group. The increase in phosphate element in the T8 group compared with the control group (Figure 4) could correspond to the stiffening of the meniscus at the microscale. These microbiomechanical alterations might directly change the macromechanical properties and the load-bearing capacity of the meniscus and further influence the loading distribution on the cartilage surface and accelerate the OA progression.

As shown in Figure 5, the Gaussian distribution of the transection group was apparently wider than that of the control groups, suggesting a

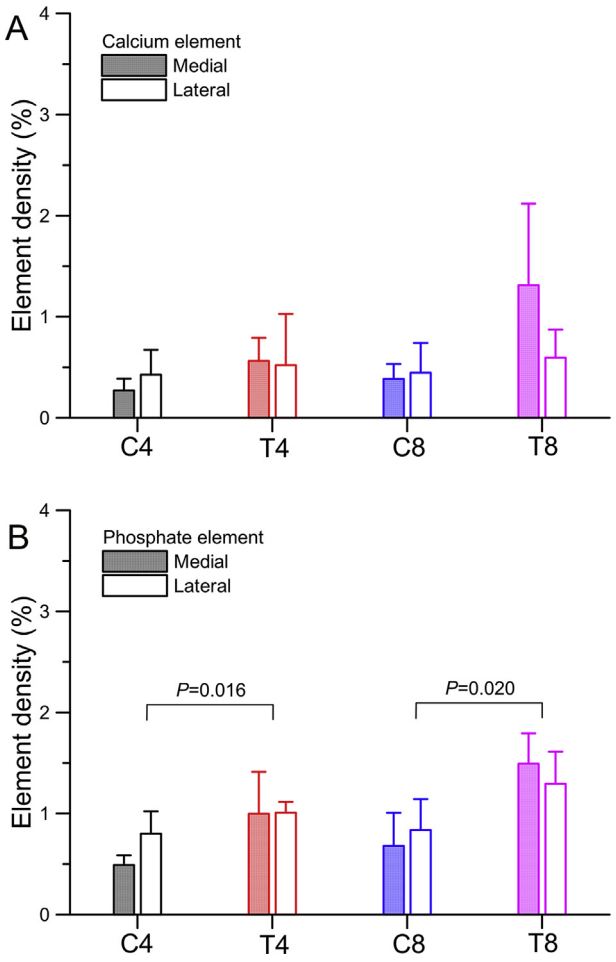

Figure 4. (A) The energy-dispersive spectrometry results of calcium in both control and transection groups; (B) the energy-dispersive spectrometry results of phosphate element in both control and transection groups (n = 5, mean ± SD). SD = standard deviation.

less uniform variation within the meniscus section [31]. The significant larger modulus of the peak position of the Gaussian curve of the T4 and T8 group in Figure 6 indicated that the alteration of biomechanical properties started on the top and bottom layers, which was associated with meniscus overloading after ACLT and severe friction between femoral cartilage and the meniscus and between the meniscus and tibial cartilage. In regard to the T8 group, the modulus of the peak position of the Gaussian curve was larger in all regions, indicating that the stiffening was expanded from the top and bottom layers towards the middle part and then resulted in whole stiffening of the lateral meniscus. In this study, the medial meniscus changed more than the lateral one, which corresponded to the stress distribution within the knee joint after ACLT, and the higher portion of medial meniscus tear in all meniscus damage [32]. The microbiomechanical alterations might directly change the macromechanical properties and the load-bearing capacity of the meniscus and further influence the loading distribution on the cartilage surface and accelerate OA progression. Because medial and lateral menisci differ in shapes, connections to the surrounding tissues, load-bearing capacity [22], and the number of tears on the medial side are significantly greater compared with the lateral side [32]. Within the interior of the meniscus, the different collagen fibre alignments and collagen types between the inner and outer regions result in a different load-bearing capacity [33,34], as shown by the most common type of tear in the peripheral posterior horn of the medial meniscus [32].

The modulus increased after ACLT with different degrees among different scanning sites, which was in agreement with a previous research study in the human meniscus at a microscale [13]. However, the alteration trend in this study was inconformity with the macrobiomechanical changes in the rabbit [27]. The different severities of OA or the spatial heterogeneity may also lead to the difference in mechanical changes. Therefore, the correlation between the microscale and macroscale in different loading directions should be further investigated. The detailed modulus at the microscale within the meniscus section may provide data for the finite element modelling study [35,36] to predict the mechanics in OA and tissue-engineering research [37,38] to improve the microstructure and micromechanics.

The elastic modulus of the intact meniscus measured in this study was in the range of 30–100 kPa. Micromechanical properties of the rabbit meniscus have not been widely reported yet. However, the modulus of the meniscus in rabbits can be compared with other species. The modulus in the mature porcine meniscus was in the range of 27.5 ± 8.8 kPa in the inner region and 151.4 ± 38.2 kPa in the outer region in the pericellular matrix [15]. The modulus in the human meniscus was in the range of 70–90 kPa in the inner region, whereas that in the outer region was 130–150 kPa [13]. The modulus in 12-week-old murine menisci was 6.1 ± 0.8 MPa [14]. Rabbit menisci have a similar modulus in magnitude to the human meniscus, suggesting that the animal model used in this study was broadly reliable.

However, this study has some limitations. One is the difference between a rabbit meniscus and the human one regarding their different biomechanical properties and molecular composition. In addition, considering the anisotropic biomechanical property of the meniscus

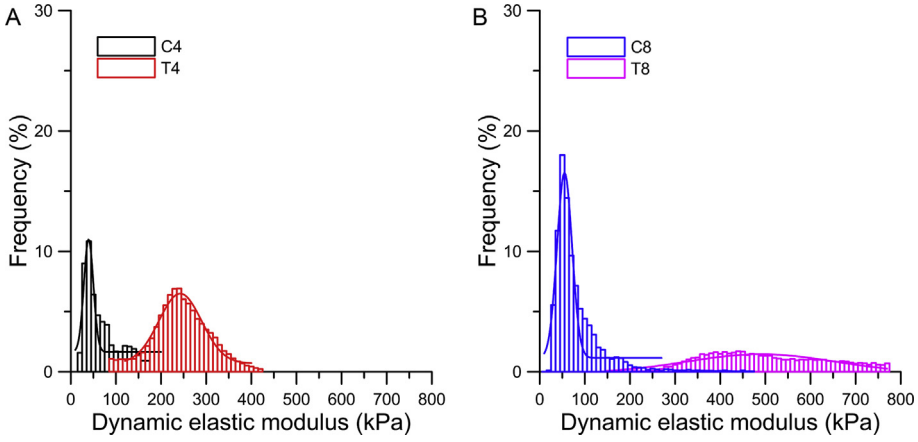

Figure 5. The representative dynamic elastic modulus in the middle site of the top layer in the medial meniscus of both control and transection groups using histogram and Gaussian distribution (n = 5, mean ± SD). (A) The dynamic elastic modulus in the middle site of the top layer in the medial meniscus of C4 and T4 groups using histogram and Gaussian distribution. (B) The dynamic elastic modulus in the middle site of the top layer in the medial meniscus of C8 and T8 groups using histogram and Gaussian distribution. SD = standard deviation.

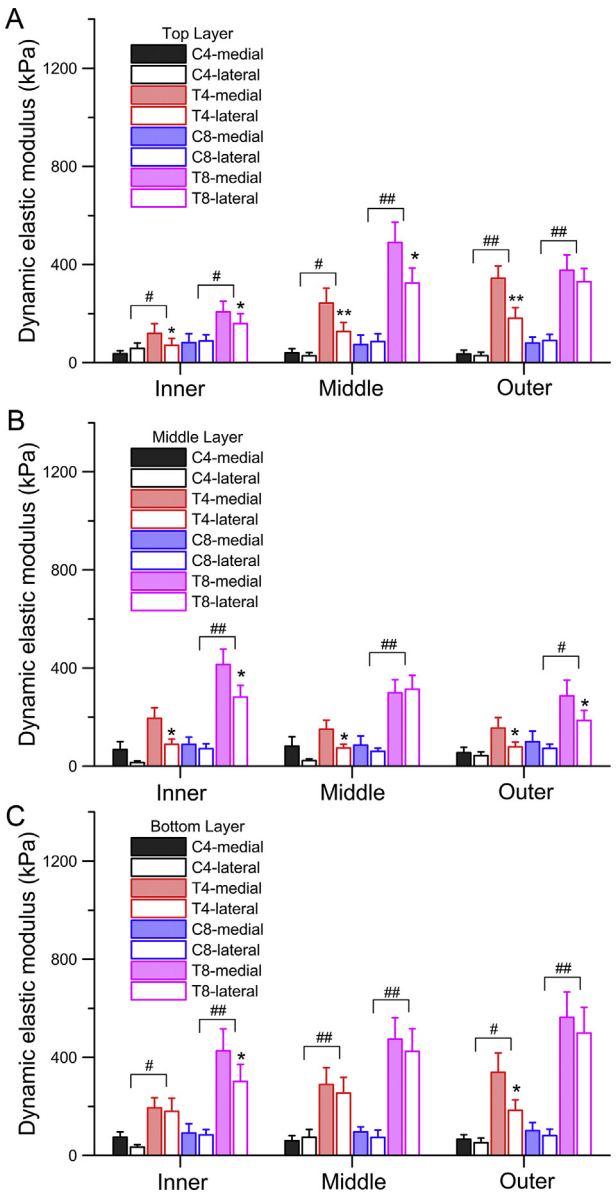

Figure 6. (A) The comparison of average dynamic elastic modulus in the top layer in both control groups and transection groups; (B) the comparison of average dynamic elastic modulus in the middle layer; (C) the comparison of average dynamic elastic modulus in the bottom layer in both control groups and transection groups. # denotes significant difference between the different transection groups ($P < 0.05$), and ## denotes a P value less than 0.001. * denotes significant difference between the lateral and medial meniscus ($P < 0.05$), and ** denotes a P value less than 0.001.

[39], the loading direction in this work also differed from the physiological loadings experienced in the human meniscus. Thus, the biomechanical properties of the meniscus in future studies should be investigated using models that resemble human physiology more accurately.

Conclusion

Microbiomechanical properties, elastic modulus, were altered to different degrees among different scanning regions sites in the early degenerative meniscus. Microbiomechanical changes occurred before the macrodegeneration signs observed by Safranin Orange/Fast Green staining. Thus, they provide a better understanding of the disease process affecting the meniscus. These microbiomechanical alterations might directly change the mechanical environment around the cells, the macromechanical properties, and the load-bearing capacity of the meniscus. Our results might be beneficial to understand how mechanical forces distribute throughout the healthy and pathologic joint. They indicate the possibility of early diagnosis using a minimally invasive arthroscopic tool, as well as they might guide the treatment to the healthy and pathologic meniscus and joint.

Funding

This work is supported by the Basic Research Program of Jiangsu Province (grant number: BK20180196), Natural Science Foundation of the Jiangsu Higher Education Institutions of China (grant number: 18KJB180024), Jiangsu Planned Projects for Postdoctoral Research Funds (grant number: 1601051C), National Natural Science Foundation of China (grant numbers: 81320108018, 31570943, and 31270995), Innovation and Entrepreneurship Program of Jiangsu Province, and the Priority Academic Program Development of Jiangsu Higher Education Institutions.

Conflict of interest

The authors have no conflicts of interest to disclose in relation to this article.

Author contributions

T.L., H.-L.Y., K.-N.A., and Z.-P.L. contributed to the conception and design of the study. T.L., H.-Y.J., H.-T.L., and Y.-J.C. contributed to the acquisition of data. T.L. and H.-Y.J. contributed to the analysis and/or interpretation of data. T.L. contributed to drafting of the manuscript. T.L. and Z.-P.L. contributed to revising the manuscript critically for important intellectual content. T.L., H.-Y.J., H.-T.L., Y.-J.C., H.-L.Y., K.-N.A., and Z.-P.L. approved the version of the manuscript to be published.

References

[1] Ahmed A, Burke D. In-vitro of measurement of static pressure distribution in synovial joints—Part I: tibial surface of the knee. J Biomech Eng 1983;105(3):216–25.
[2] Kurosawa H, Fukubayashi T, Nakajima H. Load-bearing mode of the knee joint: physical behavior of the knee joint with or without menisci. Clin Orthop Relat Res 1980;149:283–90.
[3] Cooper C, McAlindon T, Snow S, Vines K, Young P, Kirwan J, et al. Mechanical and constitutional risk factors for symptomatic knee osteoarthritis: differences between medial tibiofemoral and patellofemoral disease. J Rheumatol 1994;21(2):307–13.
[4] Bennett L, Buckland-Wright J. Meniscal and articular cartilage changes in knee osteoarthritis: a cross-sectional double-contrast macroradiographic study. Rheumatology 2002;41(8):917–23.
[5] Allaire R, Muriuki M, Gilbertson L, Harner CD. Biomechanical consequences of a tear of the posterior root of the medial meniscus: similar to total meniscectomy. JBJS 2008;90(9):1922–31.
[6] Baratz ME, Fu FH, Mengato R. Meniscal tears: the effect of meniscectomy and of repair on intraarticular contact areas and stress in the human knee: a preliminary report. Am J Sports Med 1986;14(4):270–5.
[7] Englund M, Roos EM, Lohmander L. Impact of type of meniscal tear on radiographic and symptomatic knee osteoarthritis: a sixteen-year followup of meniscectomy with matched controls. Arthritis Rheumatol 2003;48(8):2178–87.
[8] Katsuragawa Y, Saitoh K, Tanaka N, Wake M, Ikeda Y, Furukawa H, et al. Changes of human menisci in osteoarthritic knee joints. Osteoarthr Cartil 2010;18(9):1133–43.
[9] Yao Zl, Wang Sb, Zhang Y, Huang Wh, Shen Hy, Ma Lm, et al. Clinical significance of a novel knee joint stability assessment system for evaluating anterior cruciate ligament deficient knees. Orthop Surg 2016;8(1):75–80.
[10] Bhattacharyya T, Gale D, Dewire P, Totterman S, Gale ME, McLaughlin S, et al. The clinical importance of meniscal tears demonstrated by magnetic resonance imaging in osteoarthritis of the knee. JBJS 2003;85(1):4–9.
[11] Fithian DC, Kelly MA, Mow VC. Material properties and structure-function relationships in the menisci. Clin Orthop Relat Res 1990;252:19–31.
[12] Levillain A, Boulocher C, Kaderli S, Viguier E, Hannouche D, Hoc T, et al. Meniscal biomechanical alterations in an ACLT rabbit model of early osteoarthritis. Osteoarthr Cartil 2015;23(7):1186–93.
[13] Kwok J, Grogan S, Meckes B, Arce F, Lal R, D'Lima D. Atomic force microscopy reveals age-dependent changes in nanomechanical properties of the extracellular

matrix of native human menisci: implications for joint degeneration and osteoarthritis. Nanomed Nanotechnol Biol Med 2014;10(8):1777–85.
[14] Li Q, Doyran B, Gamer LW, Lu XL, Qin L, Ortiz C, et al. Biomechanical properties of murine meniscus surface via AFM-based nanoindentation. J Biomech 2015;48(8):1364–70.
[15] Sanchez-Adams J, Wilusz RE, Guilak F. Atomic force microscopy reveals regional variations in the micromechanical properties of the pericellular and extracellular matrices of the meniscus. J Orthop Res 2013;31(8):1218–25.
[16] Le Graverand M-PH, Vignon E, Otterness I, Hart D. Early changes in lapine menisci during osteoarthritis development: Part I: cellular and matrix alterations. Osteoarthr Cartil 2001;9(1):56–64.
[17] Le Graverand M-PH, Vignon E, Otterness I, Hart D. Early changes in lapine menisci during osteoarthritis development Part II: molecular alterations. Osteoarthr Cartil 2001;9(1):65–72.
[18] Madry H, Luyten FP, Facchini A. Biological aspects of early osteoarthritis. Knee Surg Sport Traumatol Arthrosc 2012;20(3):407–22.
[19] Spilker RL, Donzelli PS, Mow VC. A transversely isotropic biphasic finite element model of the meniscus. J Biomech 1992;25(9):1027–45.
[20] Guess TM, Thiagarajan G, Kia M, Mishra M. A subject specific multibody model of the knee with menisci. Med Eng Phys 2010;32(5):505–15.
[21] Upton ML, Guilak F, Laursen TA, Setton LA. Finite element modeling predictions of region-specific cell-matrix mechanics in the meniscus. Biomechanics Model Mechanobiol 2006;5(2):140–9.
[22] AufderHeide AC, Athanasiou KA. Mechanical stimulation toward tissue engineering of the knee meniscus. Ann Biomed Eng 2004;32(8):1163–76.
[23] Boulocher C, Duclos M-E, Arnault F, Roualdes O, Fau D, Hartmann D, et al. Knee joint ultrasonography of the ACLT rabbit experimental model of osteoarthritis: relevance and effectiveness in detecting meniscal lesions. Osteoarthr Cartil 2008;16(4):470–9.
[24] Sun Y, Mauerhan DR, Kneisl JS, Norton HJ, Zinchenko N, Ingram J, et al. Histological examination of collagen and proteoglycan changes in osteoarthritic menisci. Open Rheumatol J 2012;6:24.
[25] Pauli C, Grogan S, Patil S, Otsuki S, Hasegawa A, Koziol J, et al. Macroscopic and histopathologic analysis of human knee menisci in aging and osteoarthritis. Osteoarthr Cartil 2011;19(9):1132–41.
[26] Fischenich KM, Coatney GA, Haverkamp JH, Button KD, DeCamp C, Haut RC, et al. Evaluation of meniscal mechanics and proteoglycan content in a modified anterior cruciate ligament transection model. J Biomech Eng 2014;136(7):071001.
[27] Son M, Goodman S, Chen W, Hargreaves B, Gold G, Levenston M. Regional variation in T1ρ and T2 times in osteoarthritic human menisci: correlation with mechanical properties and matrix composition. Osteoarthr Cartil 2013;21(6):796–805.
[28] Killian ML, Isaac DI, Haut RC, Déjardin LM, Leetun D, Donahue TLH. Traumatic anterior cruciate ligament tear and its implications on meniscal degradation: a preliminary novel lapine osteoarthritis model. J Surg Res 2010;164(2):234–41.
[29] Wen C-Y, Wu C-B, Tang B, Wang T, Yan C-H, Lu W, et al. Collagen fibril stiffening in osteoarthritic cartilage of human beings revealed by atomic force microscopy. Osteoarthr Cartil 2012;20(8):916–22.
[30] Shao J, Lin L, Tang B, Du C. Structure and nanomechanics of collagen fibrils in articular cartilage at different stages of osteoarthritis. RSC Adv 2014;4(93):51165–70.
[31] Stolz M, Raiteri R, Daniels A, VanLandingham MR, Baschong W, Aebi U. Dynamic elastic modulus of porcine articular cartilage determined at two different levels of tissue organization by indentation-type atomic force microscopy. Biophys J 2004;86(5):3269–83.
[32] Smith JP, Barrett GR. Medial and lateral meniscal tear patterns in anterior cruciate ligament-deficient knees. Am J Sports Med 2001;29(4):415–9.
[33] Aspden R, Yarker Y, Hukins D. Collagen orientations in the meniscus of the knee joint. J Anat 1985;140(Pt 3):371.
[34] Mcdevitt CA, Webber RJ. The ultrastructure and biochemistry of meniscal cartilage. Clin Orthop Relat Res 1990;252:8–18.
[35] Pena E, Calvo B, Martinez M, Palanca D, Doblaré M. Finite element analysis of the effect of meniscal tears and meniscectomies on human knee biomechanics. Clin Biomech 2005;20(5):498–507.
[36] Peña E, Calvo B, Martinez MA, Palanca D, Doblaré M. Why lateral meniscectomy is more dangerous than medial meniscectomy. A finite element study. J Orthop Res 2006;24(5):1001–10.
[37] Makris EA, Hadidi P, Athanasiou KA. The knee meniscus: structure–function, pathophysiology, current repair techniques, and prospects for regeneration. Biomaterials 2011;32(30):7411–31.
[38] Yan L-P, Oliveira JM, Oliveira AL, Caridade SG, Mano JF, Reis RL. Macro/microporous silk fibroin scaffolds with potential for articular cartilage and meniscus tissue engineering applications. Acta Biomater 2012;8(1):289–301.
[39] Chia HN, Hull M. Compressive moduli of the human medial meniscus in the axial and radial directions at equilibrium and at a physiological strain rate. J Orthop Res 2008;26(7):951–6.